



HAL
open science

A parameterization of broadband conversion factors for Meteosat visible radiances

J. Stum, Bernard Pinty, Ramond D.

► To cite this version:

J. Stum, Bernard Pinty, Ramond D.. A parameterization of broadband conversion factors for Meteosat visible radiances. *Journal of Climate and Applied Meteorology*, 1985. hal-01978531

HAL Id: hal-01978531

<https://uca.hal.science/hal-01978531>

Submitted on 11 Jun 2021

HAL is a multi-disciplinary open access archive for the deposit and dissemination of scientific research documents, whether they are published or not. The documents may come from teaching and research institutions in France or abroad, or from public or private research centers.

L'archive ouverte pluridisciplinaire **HAL**, est destinée au dépôt et à la diffusion de documents scientifiques de niveau recherche, publiés ou non, émanant des établissements d'enseignement et de recherche français ou étrangers, des laboratoires publics ou privés.

A Parameterization of Broadband Conversion Factors for METEOSAT Visible Radiances

J. STUM, B. PINTY AND D. RAMOND

L.A.M.P./I.O.P.G., Université de Clermont II, LA/CNRS n°267, 63170 Aubière, France

(Manuscript received 13 November 1984, in final form 15 July 1985)

ABSTRACT

The conversion of radiances measured by the METEOSAT visible channel into broadband radiances can be performed as long as the appropriate conversion factors are known. A simple model allowing a spectral description of the optical properties of cloud free atmospheres and land surfaces is used to estimate these conversion factors. A sensitivity study of these factors indicates that a knowledge of the optical properties of the surfaces (described through spectrally averaged albedos and spectral band ratios) is decisive for retrieving broadband conversion factors. A parameterization is proposed which permits estimation of METEOSAT conversion factors for radiation budget calculations.

1. Introduction

For several years, satellite data have been commonly used in earth radiation budget studies. Considering the studies devoted to the part of the budget occurring in the visible range, which is the main concern of this paper, a difficulty has been often encountered as to the generalization of the results due to inherent limitations inferred by the design of the satellite system that is used in each of these studies (e.g., use of flat plate or scanning detectors, sunsynchronous or geosynchronous orbits, narrow or broadband sensing instruments). In particular, the attainable accuracy of the radiation budget quantities derived from the present operational geostationary satellites in the visible range is obviously limited by the fact that the total range is only sampled over a narrow band.

Visible channels of the European METEOSAT 1 and 2 satellites suffer from this drawback. As mentioned by Stephens *et al.* (1981), the measurements in the visible range require corrections to get broadband total shortwave radiances. The METEOSAT 2 visible channel has been calibrated by Kriebel (1983) by comparison with the data of a 0.3–3 μm pyroelectric detector on board a high-flying aircraft. These calibrations refer to a region located in Spain and to a desert in Tunisia. From radiation transfer calculations, Möser *et al.* (1980) have investigated the conversion of filtered to unfiltered radiances over the Sahara desert. Obviously, the results of these analyses cannot be straightforwardly extended to other areas imaged under different atmospheric and geometric conditions. Using a more extensive theoretical approach, Koepke (1983) analyzed the variability of the conversion factor between unfiltered and filtered radiances over a large set of surface reflectance, atmospheric state and relative observational geometry. He showed that the variation

of the conversion factor over a surface could reach ± 1 around average values of 2.8 and 2.4 for vegetated and bare surfaces respectively. So, the retrieval of unfiltered radiances appears to be very hazardous for a given region imaged at a given time under unknown detailed atmospheric conditions.

The purpose of this paper is to examine quantitatively the sensitivity of the conversion factor applicable to the METEOSAT 1 and 2 visible channels with respect to the main parameters involved; these are the angles of the sun and satellite, the optical properties of the atmosphere and those of the underlying surface. Our investigation, which is limited to cloud free cases, uses a simplified spectral description of the radiative transfer in the atmosphere and of the surface conditions. To provide simple and suitable correction of the radiances measured by METEOSAT within the visible range, a parameterization of the conversion factor is proposed in section 5.

2. METEOSAT conversion factors

The effective radiance L_{SAT} measured by METEOSAT is the integral of the spectral radiance $L_{T\lambda}$ leaving the top of the atmosphere weighted with the spectral response of the METEOSAT visible channel $\tau_{\text{SAT}\lambda}$:

$$L_{\text{SAT}} = \int_0^{\infty} L_{T\lambda} \tau_{\text{SAT}\lambda} d\lambda. \quad (1)$$

The nearly triangular shape of the spectral response $\tau_{\text{SAT}\lambda}$ of the METEOSAT 1 visible channels is shown in Fig. 1 (Morgan, 1981). It extends from 0.4 to 1.1 μm with a maximum response at 0.725 μm .

According to Koepke (1982), the effective radiance L_{SAT} can be used to determine the total radiance L_{SOL} over the solar visible spectrum for use in radiation

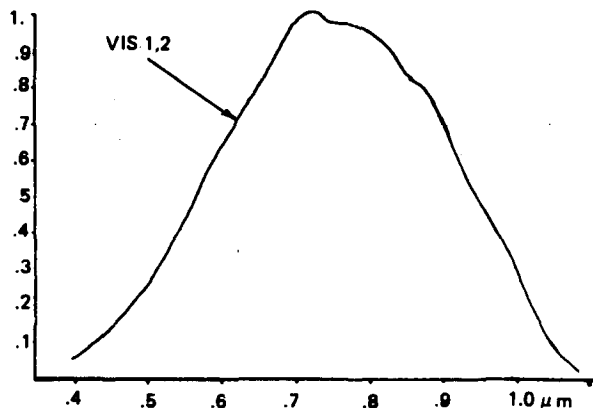


FIG. 1. Normalized spectral response of the two identical visible channels of METEOSAT 1 (from Morgan, 1981).

budget studies. This determination can be made simply by multiplying L_{SAT} by an appropriate conversion factor F_{SOL} :

$$L_{SOL} = \int_{0.2 \mu m}^{4 \mu m} L_{T\lambda} d\lambda = L_{SAT} F_{SOL}. \quad (2)$$

Obviously, F_{SOL} has to account for all the observational conditions that may influence the relative distribution of the radiance $L_{T\lambda}$ over the shortwave solar range. More precisely, F_{SOL} has to account for the variability of the observational geometry parameters, the atmospheric radiative state, and the optical properties of the underlying surface itself. Thus, as stated by Koepke (1982), as long as the optically relevant parameters are known, the radiance $L_{T\lambda}$ over the broad band spectral range can be computed and the conversion factor can be determined.

3. Specifications of atmospheric and surface optical properties

Our main concern here is to describe representative trends rather than to accurately evaluate the influence of specific atmospheric characteristics on the radiances reaching the sensor. Then, the calculation of the radiance $L_{T\lambda}$ leaving the atmosphere has been performed through a simplified spectral model where in particular multiple scattering and aerosol absorption are neglected. This simplification may seem quite rough, but the use of a more sophisticated model may not be necessary in the present state of art as long as the complete knowledge of the detailed optical properties of the atmosphere cannot be achieved on a global scale, as noted by Slater and Jackson (1982).

According to Deschamps *et al.* (1983), the monochromatic radiance $L_{T\lambda}$ over a uniform surface of large size can be approximated as follows:

$$L_{T\lambda} \approx T_g[L_{a\lambda} + L_\lambda T(\theta_v)], \quad (3)$$

where $L_{a\lambda}$ is the intrinsic atmospheric radiance, L_λ is the radiance reflected by the surface at ground level, $T(\theta_v)$ is the total transmission factor of the scattering atmosphere, θ_v is the satellite viewing angle, and T_g is the total transmission factor for gaseous absorption.

In Eq. (3) it is assumed that the gaseous absorption takes place in layers located above those where atmospheric scattering is effective. Spectral absorption by water vapor and ozone has been taken into account by means of a parameterization scheme adapted from the LOWTRAN IV B code by Selby *et al.* (1978). The resulting atmospheric transmission for spectral absorption takes the form:

$$T_g(\lambda, U) = \exp[-P(\lambda)U^n],$$

with $n = 0.5$ and $n = 1$ for water vapor and ozone absorption, respectively, U is the gas concentration and $P(\lambda)$ is a polynomial, the coefficients of which have been adjusted according to a fitting procedure.

This study uses the description of the optical properties of nonabsorbing aerosols proposed by McClatchey *et al.* (1971). The real refractive index is taken equal to 1.5 and only single scattering is considered. If the optical thicknesses for molecular and aerosol scatterings τ_R and τ_A are known, the total transmission factor can be expressed (Deschamps *et al.*, 1983) by:

$$T(\theta_v) \approx (1 + b\tau/\cos\theta_v)^{-1}, \quad (4)$$

with $b\tau = 0.5\tau_R + 0.16\tau_A$ and $b = (1 - g)/2$, g the phase function asymmetry factor and τ the total optical thickness of scattering atmosphere. A discussion of the above approximations can be found in Tanré *et al.* (1979). The $1 \mu m$ aerosol optical depth is specified through the ground visibility (Deschamps *et al.*, 1981).

If single scattering is considered, the intrinsic atmospheric radiance can be approximated as follows:

$$L_{a\lambda} \approx (E_0 \cos\theta_s/\pi)(\tau P/4 \cos\theta_s \cos\theta_v), \quad (5)$$

where $\tau P = \tau_R P_R + \tau_A P_A$, E_0 is the solar irradiance at the top of the atmosphere, θ_s the solar zenith angle, and P_R and P_A are the Rayleigh and aerosol scattering phase functions, respectively.

With the same definitions, the radiance L_λ is given by:

$$L_\lambda \approx E_0 \cos\theta_s/\pi [T(\theta_s)\rho/(1 - \rho s)], \quad (6)$$

where $s \approx 2b\tau/(1 + 2b\tau)$ is the spherical albedo of the scattering atmosphere and ρ is the surface reflectance.

In the present study, the optical properties of the surfaces are specified by the spectrally averaged albedo $\bar{\rho}$ defined by:

$$\bar{\rho} = \frac{\int_{0.2 \mu m}^{4 \mu m} \rho(\lambda) E_G(\lambda) d\lambda}{\int_{0.2 \mu m}^{4 \mu m} E_G(\lambda) d\lambda}, \quad (7)$$

where $E_G(\lambda)$ is the surface spectral irradiance and $\rho(\lambda)$ the spectral albedo of the surface. Since most land surfaces are characterized by an increasing albedo in the near infrared, the additional surface parameter I has been used:

$$I = (\rho_2 - \rho_1)/(\rho_2 + \rho_1). \quad (8)$$

For the definition of the above surface parameter I , the spectral distributions of the albedo over the visible and near infrared ranges is assimilated to a step function. The jump occurs at the wavelength λ^* ; ρ_1 is the value of the mean albedo over the shortwave part of the spectrum ($\lambda < \lambda^*$) and ρ_2 is the value of the longwave part of the spectrum ($\lambda > \lambda^*$, $\rho_2 \geq \rho_1$).

The parameter I has the same form as the spectral band ratios currently in use in remote sensing for scene classification or ground signature from the actual multispectral radiometers (e.g., vegetation index from AVHRR). In the following, λ^* will take the value 0.6, 0.7 or 0.8 μm .

4. METEOSAT conversion factor behavior

As mentioned in section 2, the METEOSAT conversion factor depends on the relative distribution of the radiance $L_{T\lambda}$ over the solar shortwave spectral range. The occurrence of relatively high $L_{T\lambda}$ values near the maximum response of the METEOSAT visible channel leads to small conversion factors; on the opposite, the conversion factor takes high values when the highest spectral radiances $L_{T\lambda}$ are located away from the maximum response of the sensor.

As examples of the results of the sensitivity analysis, Figs. 2–5 show the variations of F_{SOL} for different surface and atmospheric conditions and for various geometrical parameters. In Fig. 2, F_{SOL} is plotted against surface albedo (constant with wavelength) for a set of extreme atmospheric conditions. From this figure, a general decrease of F_{SOL} with an increasing albedo is observed. It results from a decrease of the relative contribution of the sky signal to the total signal with increasing surface albedo values. Indeed, over low albedo surfaces and due to the atmospheric scattering, relatively high values of the spectral radiances $L_{T\lambda}$ are located at wavelengths shorter than that where the maximum of the response function of the sensor occurs, which yields high values of F_{SOL} . As seen in Fig. 2, water vapor absorption acts to reduce the F_{SOL} factor and especially over high albedo surfaces. Since water vapor absorption occurs at wavelengths greater than 0.7 μm , L_{SAT} values are relatively less reduced than are the L_{SOL} values and this effect is enhanced by an increasing albedo. The decrease rate of the conversion factor with an increasing albedo is reduced if a rather turbid atmosphere (5 km visibility) is considered, especially for low albedo values. Indeed, under such atmospheric conditions, the radiances within the METEOSAT visible channel become comparatively higher than for clearer sky cases. Analogous conclusions have

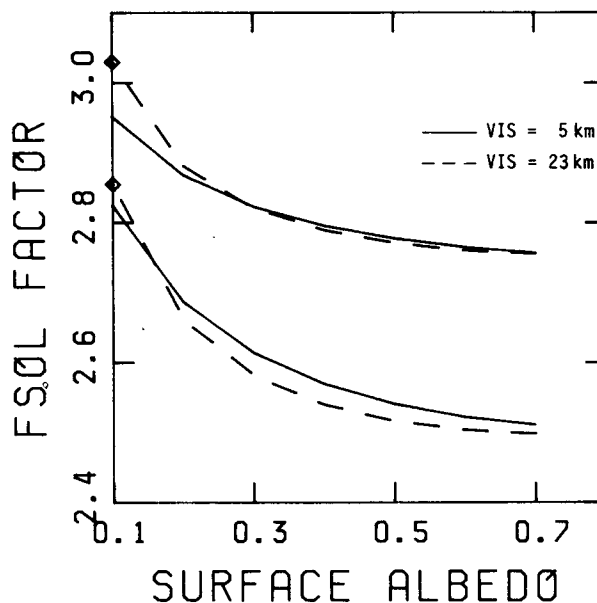


FIG. 2. Conversion factor F_{SOL} against surface albedo (constant over wavelength) for two values of ground visibility VIS. The two upper curves are for a precipitable water content $U_{H_2O} = 0$ cm; the two lower curves are for $U_{H_2O} = 5$ cm. In both cases, the solar and satellite zenith angles are 15° , the relative azimuth angle is 0° and the total amount of ozone is 0.25 atm cm.

been previously underlined by Koepke (1982) when discussing F_{SOL} values over various colored oceans.

Figure 3 shows the effect of an increasing solar zenith angle. The behavior of F_{SOL} results mainly from the shift of the radiance distribution towards shorter wavelengths due to stronger scattering. The dependency of F_{SOL} on solar zenith angle is reduced over high albedo surfaces (lower curves) due to the decrease of the relative contribution of the sky radiance to the total signal.

The dependency of F_{SOL} on the spectral band ratio I , when λ^* equals 0.7 μm , is illustrated in Fig. 4. The small decrease rate of F_{SOL} with an increasing I is a common feature of the six given curves. Since for a constant average albedo an increase of the spectral band ratio corresponds to a lower albedo in the range 0.2–0.7 μm and to a higher albedo in the range 0.7–4 μm , the effects due to water vapor absorption and scattering counteract each other. As already explained for Fig. 2, absorption tends to decrease F_{SOL} with an increasing I whereas scattering tends to increase F_{SOL} with an increasing I . The resulting decrease in F_{SOL} shown in Fig. 4, which is larger for high albedos and low turbidity, indicates that water vapor absorption is predominant over scattering as far as the behavior of F_{SOL} is concerned.

The influence of the color of the underlying surface on F_{SOL} behavior is illustrated in Fig. 5. In this figure, for an averaged albedo equal to 0.3, three different values of λ^* are considered and in each case the METEOSAT conversion factor is plotted against the spectral

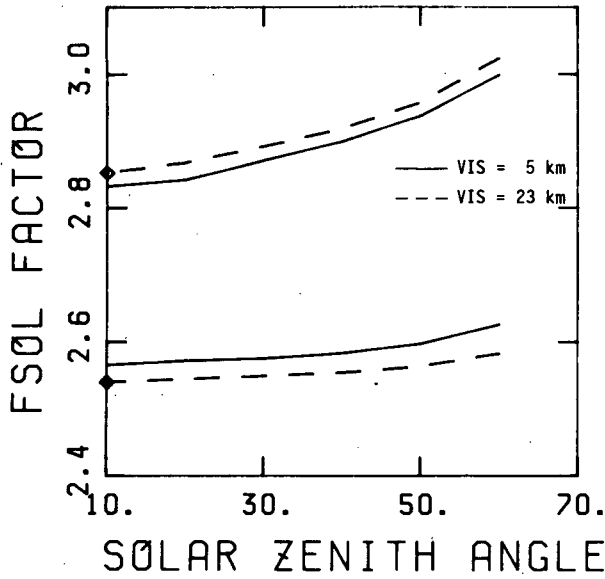


FIG. 3. Conversion factor F_{SOL} against the solar zenith angle for two values of ground visibility VIS . The two upper curves are for a surface albedo $\bar{\rho}$ (constant over wavelength) = 0.1; the two lower curves are for $\bar{\rho}$ = 0.4. In both cases the precipitable water content is 3 cm. Other parameters are the same as in Fig. 2.

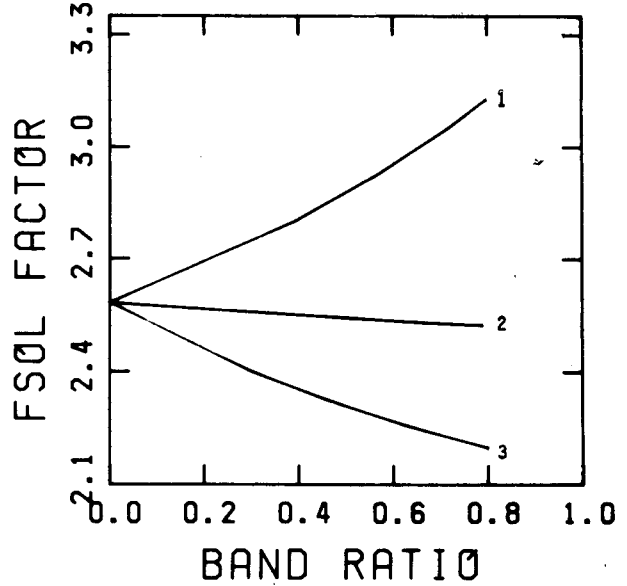


FIG. 5. Conversion factor F_{SOL} against the spectral band ratio I (see Eq. (8)) for three values of λ^* . Curves 1, 2 and 3 are for λ^* equal to 0.8 μm , 0.7 μm and 0.6 μm , respectively. In each case, the averaged surface albedo $\bar{\rho}$ is 0.3 and the ground visibility VIS is 23 km. Other parameters are the same as in Fig. 3.

band ratio. As already seen from Fig. 4, the variation of F_{SOL} with the spectral band ratio is low if λ^* equals 0.7 μm . However, Fig. 5 reveals completely different variations for F_{SOL} values when slight spectral shifts in λ^* values occur. Since the METEOSAT visible channel

has a spectral response from about 0.4 to 1.1 μm with a maximum near 0.7 μm , a shift of λ^* towards lower values than 0.7 μm yields, for a constant averaged albedo, comparatively higher radiances within the visible channel, which results in a smaller F_{SOL} factor. A shift of λ^* to 0.8 μm (upper curve) yields, on the contrary, higher F_{SOL} values. Obviously, the influence of the color of the surface on the METEOSAT radiance is enhanced by an increase of the spectral band ratio. It is important to note that, under medium atmospheric conditions, the value of λ^* , i.e., the wavelength where a step increase of the albedo occurs in the near infrared, plays a crucial role for METEOSAT F_{SOL} behavior.

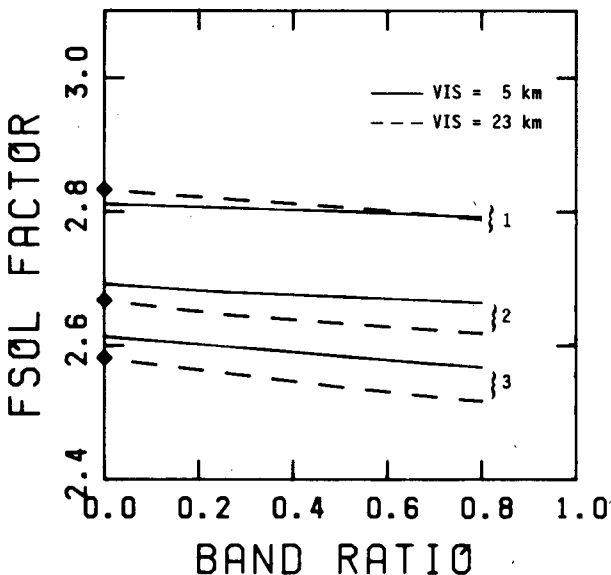


FIG. 4. Conversion factor F_{SOL} against the spectral band ratio I [see Eq. (8)] with $\lambda^* = 0.7 \mu\text{m}$, for two values of ground visibility VIS . Curves referred to as 1, 2, 3 correspond to averaged surface albedos of 0.1, 0.2 and 0.3, respectively. Other parameters are the same as in Fig. 3.

5. Parameterization of METEOSAT conversion factors

For application to radiation budget calculations for instance, it is desirable to get an expression which allows the retrieval of METEOSAT conversion factors from the major optical parameters of the atmosphere and surface. Furthermore, the involved parameters must be known or estimated on a routine basis either from surface, upper-air or satellite observations, or from climatological data. It is proposed here to express the F_{SOL} factor as a function of seven such parameters, namely, the solar zenith angle θ_s , the satellite viewing angle θ_v , the declination of the sun δ , the ground visibility VIS , the water vapor content U_{H_2O} , the averaged albedo $\bar{\rho}$ and the spectral band ratio I . The latitude, longitude and declination of the sun have been used

in place of the relative azimuth angle because this parameter varies with θ_s . From the large variety of data sets that were tested in the sensitivity study, it has been found that the dependency of F_{SOL} with the total ozone content was negligible; in the computation of the parameterized expression of F_{SOL} , the total ozone content has been assumed constant and equal to 0.25 atm cm, and the longitude was kept constant and equal to 0° . Among the seven explicit parameters retained heretofore for an attempt to parameterize F_{SOL} , λ^* does not appear though it has been shown that λ^* may play a crucial role. This choice has been made because λ^* cannot be presently assessed on an operational basis on the desired scale. It is certainly the major, but unavoidable, drawback of the proposed parameterization. In the computation leading to the parameterized expression of F_{SOL} , λ^* is assumed constant and equal to $0.7 \mu\text{m}$. This value of $0.7 \mu\text{m}$ presents, at least, the advantage that first, the corresponding spectral band ratios can be estimated from AVHRR data, and second, that in many climate models the increase step of albedo in the near infrared over the snow-free land is assumed to occur at $0.7 \mu\text{m}$ (Henderson-Sellers and Wilson, 1983).

Although the intervening variables are not strictly independent, a Taylor's expansion has been used to develop the F_{SOL} factor with respect to the chosen parameters. In order to simplify the parameterization, all

the crossed partial derivatives in the expansion have been neglected. After calculation of an average F_{SOL} value from a set of values of the parameters that minimize the contributions of neglected effects, each curve relating significant F_{SOL} variations with the intervening parameters has been fitted with polynomials. The following expression has been obtained:

$$F_{SOL} = 2.648 + f_1(\theta_s - 20^\circ) + f_2(\theta_v - 23^\circ) + f_3(\delta - 21^\circ) + f_4(\text{VIS} - 20 \text{ km}) + f_5(U_{H_2O} - 3 \text{ cm}) + f_6(\bar{\rho} - 0.2) + f_7(I). \quad (9)$$

Table 1 gives the order and the coefficients of each polynomial f_j with the range of variable values for which Eq. (5) can be used.

To estimate the errors due to the parameterization itself, we computed F_{SOL} factors within a 50° great-circle arc of the subsatellite point using the model described in section 3 and we compared these values with those derived from Eq. (9) for several data sets of atmospheric and surface conditions and geometrical parameters. As expected, and mainly as a result of neglecting second order effects, the largest differences did not exceed ± 0.1 and only occurred with data sets which corresponded to the highest and lowest F_{SOL} values, respectively.

TABLE 1. Order and coefficients of polynomial expressions f_j corresponding to the expansion for the METEOSAT conversion factor $F_{SOL} = 2.648 + \sum_{j=1}^7 f_j(x_j)$.

Variable (x_j)	Order N of $f_j(x_j) = \sum_{i=1}^N a_i x_j^i$	Coefficients (a_i)	Exponents (i)	Validity range for the variables
$\theta_s - 20$	4	-0.6722 E - 04	1	$0 < \theta_s < 60^\circ$
		-0.2050 E - 05	2	
		0.2055 E - 06	3	
		0.1668 E - 07	4	
$\theta_v - 23$	4	0.1140 E - 02	1	$0 < \theta_v < 57^\circ$
		0.6361 E - 04	2	
		0.7794 E - 06	3	
		0.2062 E - 07	4	
$\delta - 21$	2	-0.1343 E - 02	1	$-23.45^\circ < \delta < 23.45^\circ$
		0.1204 E - 04	2	
VIS - 20	2	-0.1262 E - 02	1	$5 < \text{VIS} < 30 \text{ km}$
		0.4215 E - 04	2	
$U_{H_2O} - 3$	2	-0.4061 E - 02	1	$1 < U_{H_2O} < 6 \text{ cm}$
		0.1252 E - 02	2	
I	2	-0.6957 E - 01	1	$0 < I < 1$
		0.1784 E - 01	2	
$\bar{\rho}$	4	-0.1254 E + 01	1	$0.1 < \bar{\rho} < 0.7$
		0.5477 E + 01	2	
		-0.1267 E + 02	3	
		0.1097 E + 02	4	

6. Conclusions

The behavior of METEOSAT conversion factors has been examined for the cloud free cases over land without snow with respect to the more sensible optical parameters. It has been confirmed that, under medium atmospheric conditions and for low zenith angles of sun and satellite, the conversion factor is mainly sensitive to the optical properties of the underlying surface.

A parameterization of the conversion factor has been derived which allows a first estimate of the radiance at the satellite in the total solar range which can be worthwhile in radiation budget studies using METEOSAT data. The choice of the explicit parameters has been arbitrarily limited to those which can be obtained on a routine basis or from climatological data. The consequences of this choice are that the proposed parameterization uses rough representation of atmospheric and surface properties, and may not be adapted to more specific atmospheric and/or surface conditions. A major limitation exists for surfaces which exhibit a near infrared increase of the spectral albedo at a wavelength departing from $0.7 \mu\text{m}$. However, significant improvements of such parameterization are conditioned at first by the availability over large regions of reliable data concerning the main optical parameters.

Acknowledgments. The authors would like to thank Drs. P. Koepke and K. T. Kriebel for reading the manuscript and for helpful suggestions. Special thanks are also due to Drs. H. Isaka, Y. Pointin and G. Szejwach for their interest and advice. The authors are indebted to R. Pejoux for his assistance in programming. They are also grateful to C. Paquet for typing the manuscript and J. Squarise for editing aid.

REFERENCES

- Deschamps, P. Y., M. Herman and D. Tanré, 1981: Influence de l'atmosphère en télédétection des ressources terrestres. Modélisation et possibilités de correction. *Signatures Spectrales d'Objets en Télédétection*, Avignon, 674 pp.
- , — and —, 1983: Definitions of atmospheric radiance and transmittances in remote sensing. *Remote Sens. Environ.*, **13**, 89–92.
- Henderson-Sellers, A., and M. F. Wilson, 1983: Surface albedo data for climatic modeling. *Rev. Geophys. Space Phys.*, **21**, 1743–1778.
- Koepke, P., 1982: Vicarious satellite calibration in the solar spectral range by means of calculated radiances and its application to METEOSAT. *Appl. Opt.*, **21**, 2845–2854.
- , 1983: Calibration of the vis-Channel of METEOSAT 2. *Advanced Space Research*, **2**, 93–96.
- Kriebel, K. T., 1983: Results of METEOSAT-2 vis-Channel calibration. *Proc. Fourth METEOSAT Scientific User Meeting*, Clermont-Ferrand, ESOC.
- McClatchey, R. A., R. W. Fenn, J. E. A. Selby, F. E. Voltz and J. S. Garing, 1971: Optical properties of the atmosphere. AFCRL 71-0279, Environ. Res. Pap. 354, Hanscom AFB, MA.
- Morgan, J., 1981: Introduction to the METEOSAT system. MDMD, ESOC.
- Möser, W., H. J. Preuss, E. Raschke and E. Ruprecht, 1980: Determination of radiation balance parameters using METEOSAT image data—preliminary studies. *Proc. Second METEOSAT Scientific User Meeting*, London, ESOC.
- Selby, J. E. A., F. X. Kneizys, J. H. Chetwynd and R. A. McClatchey, 1978: Atmospheric transmittance/radiance: Computer code LOWTRAN 4. AFGL-TR-78-0053, Air Force Geophysics Laboratory, Hanscom AFB, MA.
- Slater, P. N., and R. D. Jackson, 1982: Atmospheric effects on radiation reflected from soil and vegetation as measured by orbital sensors using various scanning conditions. *Appl. Opt.*, **21**, 3923–3931.
- Stephens, G. L., G. G. Campbell and T. H. Vonder Haar, 1981: Earth radiation budget. *J. Geophys. Res.*, **86**, 9739–9760.
- Tanré, D., M. Herman, P. Y. Deschamps and A. de Leffe, 1979: Atmospheric modeling for space measurements of ground reflectances, including bidirectional properties. *Appl. Opt.*, **18**, 3587–3594.